Division of Geological & Geophysical Surveys

PUBLIC-DATA FILE 97-43

PORTFOLIO OF AEROMAGNETIC AND RESISTIVITY MAPS OF THE STIKINE AREA, SOUTHEAST ALASKA

by

Laurel E. Burns

and

Shirley A. Liss

October 1997

Released by

STATE OF ALASKA
DEPARTMENT OF NATURAL RESOURCES
Division of Geological & Geophysical Surveys
794 University Avenue, Suite 200
Fairbanks, Alaska 99709-3645

PORTFOLIO OF AEROMAGNETIC AND RESISTIVITY MAPS OF THE STIKINE AREA, SOUTHEAST ALASKA

A cooperative agreement between the Alaska Division of Geological & Geophysical Surveys (DGGS), the U.S. Department of the Interior Bureau of Land Management (BLM), and the City of Wrangell resulted in acquiring and releasing geophysical data of the Stikine area, southeast Alaska. Funding was provided by BLM and the City of Wrangell. The contract was monitored and the data published by DGGS in 1997.

This Public-data file (PDF) briefly describes the aeromagnetic and electromagnetic data and contains page-size illustrations of the data. The airborne geophysical information consists of aeromagnetic data and resistivity data at 900, 7200, and 56,000 Hz. This portfolio includes color maps of the aeromagnetic data, color maps of the coplanar resistivity data at 900 and 7200 Hz, three black & white shadow maps of the aeromagnetic maps, and an acetate overlay of the topography. PDF 97-44 gives a more detailed interpretation of the data and a more complete description of the processing. Clients can request any color map from this portfolio at scale of 1:63,360 (1 inch = 1 mile) from the Alaska Division of Geological & Geophysical Surveys, 794 University Ave., Suite 200, Fairbanks, Alaska, 99709. Phone: (907) 451-5020. FAX: (907) 451-5050. These maps are already prepared and are listed at the end of this sheet. Custom plots of variations of the data can be made at any scale at the DGGS office for a reasonable fee. Some of the products are available at the Bureau of Land Management Offices in Juneau.

The acetate topography included with this portfolio should be used only for generalized locations. For accurate locations, the large scale geophysical maps or the computer files should be used.The area surveyed includes parts of the Petersburg A-2, A-3, B-1, B-2, B-3, B-4, C-1, C-3, C-4, C-5, D-4, D-5, D-6, the Sumdum A-4, A-5, A-6, and the Bradfield Canal B-6, C-6 quadrangles.

Survey history, instrumentation, & data processing

The following indented section describing the instrumentation and processing is from the maps produced by WGM and Geoterrex-Dighem, the contractor and subcontractor, in conjunction with DGGS.

> The airborne geophysical data for the Stikine area were compiled and drawn under contract between the State of Alaska, Department of Natural Resources, Division of Geological & Geophysical Surveys, and WGM, Mining and Geological Consultants, Inc. Airborne geophysical data for the area were acquired by Geoterrex-Dighem, a division of CGG Canada Ltd., in 1997.
>
> Geophysical data were acquired with a Geoterrex-Dighem Electromagnetic (EM) system, a Scintrex cesium magnetometer, and a Herz VLF system installed in an AS350B-2 Squirrel helicopter. In addition, the survey recorded data from a radar altimeter, GPS navigation system, 50/60 Hz monitors, and a video camera. Flights

were performed at a mean terrain clearance of 200 feet along survey flight lines with a spacing of a quarter of a mile. Tie lines were flown perpendicular to the flight lines at intervals of approximately three miles.

A Sercel Real-Time Differential Global Positioning System (RT-DGPS) was used for both navigation and flight path recovery. The helicopter position was derived every 0.5 seconds using both real-time differential positioning to a relative accuracy of less than 10 m. Flight path positions were projected onto the Clark 1866 (UTM) spheroid, 1927 North American datum using a central meridian (CM) of 135 degrees, a north constant of 0 and an east constant of 500,000. Positional accuracy of the presented data is better than 10 m with respect to the UTM grid.

Total Field Magnetics:
The magnetic total field contours were produced using digitally recorded data from a Scintrex cesium magnetometer, with a sampling interval of 0.1 seconds. The magnetic data were (1) corrected for diurnal variations by subtraction of the digitally recorded base station magnetic data, (2) leveled to the tie line data, and (3) interpolated onto a regular 100 m grid using a modified Akima (1970) technique. The regional variation (or IGRF gradient, 1985 updated to October 1996) was removed from the leveled magnetic data.

Resistivity:
The Dighem^{V} EM system measured inphase and quadrature components at five frequencies. Two vertical coaxial coil-pairs operated at 900 and 5000 Hz while three horizontal coplanar coil-pairs operated at 900, 7200, and 56,000 Hz. EM data were sampled at 0.1 second intervals. For the 900 and 7200 Hz resistivity maps, the resistivity is generated from the inphase and quadrature component of the coplanar 900 and 7200 Hz respectively using the pseudo-layer half space model. The data were interpolated onto a regular 25 m grid using a modified Akima (1970) technique.

Akima, H., 1970, A new method of interpolation and smooth curve fitting based on local procedures: Journal of the Association of Computing Machinery, v. 17, no. 4, p. 589-602.

Magnetic data

The magnetometer is a passive instrument that measures the earth's magnetic field in nanoteslas (nT). Rocks with high magnetic susceptibilities (measured in SI units) locally attenuate or dampen these magnetic signals producing the relative highs and lows. Iron-rich magnetic minerals such as magnetite, ilmenite, and pyrrhotite have the highest magnetic susceptibility. These minerals commonly occur in mafic volcanic rocks (such as basalt), mafic and ultramafic plutonic rocks (such as serpentinite, clinopyroxenite, and gabbro), some skarns, and in some other geologic units. Rocks with low to no iron tend to produce little variation in the magnetic signal. These include silicic volcanic rocks (rhyolites), silicic plutonic rocks (granites), and most

sedimentary rocks (for example, limestone, sandstone, and shale). Some iron rich minerals – such as pyrite – are not magnetic and do not produce a magnetic signal.

Different types of ore deposits have different magnetic signatures. A bedrock gold deposit associated with the top of a granitic pluton would likely be an aeromagnetic low whereas a magnetite-bearing gold skarn would be an aeromagnetic high. A gold deposit hosted by a low-angle (thrust) fault has a different signature than one hosted by a high-angle fault.

Figure 1 shows the aeromagnetic data for the Stikine area. The high values (in nanoteslas) are purple and orange and indicate appreciably magnetic rocks. The low values are the blues and greens. A gradual change in color indicates a gradual change in the magnetic field strength. This can be caused by either a gradual change in magnetic susceptibility of rocks near the surface, the gradual burial of a rock unit of relatively constant magnetic susceptibility, or the introduction of a new unit at depth. Conversely, an abrupt change in color indicates an abrupt change in the magnetic susceptibility. This is caused by juxtaposing two rock units with very different magnetic susceptibilities such as is the case with faults, volcanic dikes, or some mineralized zones. Faults can be inferred on aeromagnetic maps from linear or curvilinear features composed of discontinuous aeromagnetic highs or lows.

Figures 2, and 3 show the aeromagnetic data presented as "shadow" maps. These three-dimensional maps simulate a light source shining on the data. The higher values appear bright like the mountain tops struck by sunlight. The light source can be rotated in a complete circle with 0° (north) clockwise to 180° (south) and back to 360° (north). Figure 2. shows azimuth 147° (apparent light source in the southeast), and figure 3 shows azimuth 282° (apparent light source in the northwest). Shadow maps can enhance structures, such as faults, intrusions, and the trend of stratigraphic layers.

Resistivity data

The electromagnetic (EM) system is an active instrument that measures the resistivity of the rocks below it by sending out electromagnetic signals at different frequencies and recording the signals that are returned from the earth. The high values (measured in ohm-m) are indicative of resistive (low conductivity) rocks, such as quartzite. Low resistivity (high conductivity) values are present for bedrock conductors (water-saturated clays, graphite, concentrations of certain sulfides, some alteration halos), conductive overburden (water-saturated zones), and cultural sources (e.g. powerlines). The main conductive minerals are graphite, most sulfides, (but not sphalerite), and water-saturated clays. Rocks hydrothermally altered to clay minerals also are conductive. Some faults will show up very well on the resistivity maps, because they either offer a conduit for ground water or they separate rocks with markedly different resistivities.

The EM instrument (bird) contains 5 or more transmitting coils in front and 5 matching (paired) receiver coils in the rear. Three of these pairs are coplanar – the axes of the coils are perpendicular to the long axis of the bird. Two of these pairs are coaxial – the axes of the coils are parallel to the long axis of the bird. These two major geometric configurations, coplanar and coaxial, record different information about the conductivity of the rocks below. Coplanar coils

emphasize horizontal and flat lying conductive units. Coaxial coils emphasize vertical to near vertical conductive units.

The EM coplanar coil pairs are processed to produce resistivity maps, shown in figures 4 and 5. Since ground penetration correlates inversely with frequency, the 7200 Hz reflects near surface rocks and the 900 Hz adds the influence of deeper rocks in general. However, the depth of penetration is variable depending on the resistivity of the rocks the signal is passing through. Although the color bars in these figures differ, each figure has the most conductive rocks shown as purple and orange.

Report of Investigations RI 97-16A-E and PDF 97-38A-E shows EM anomalies from coaxial pairs as circular symbols along the flight path lines. This model emphasizes "discrete" bedrock conductors. These anomalies are too numerous to place in this portfolio. PDF 97-44 gives a more detailed discussion of these EM anomalies.

The topographic map is included as figure 6. This can be used as an overlay for the data.

Location Index for scale 1:63,360

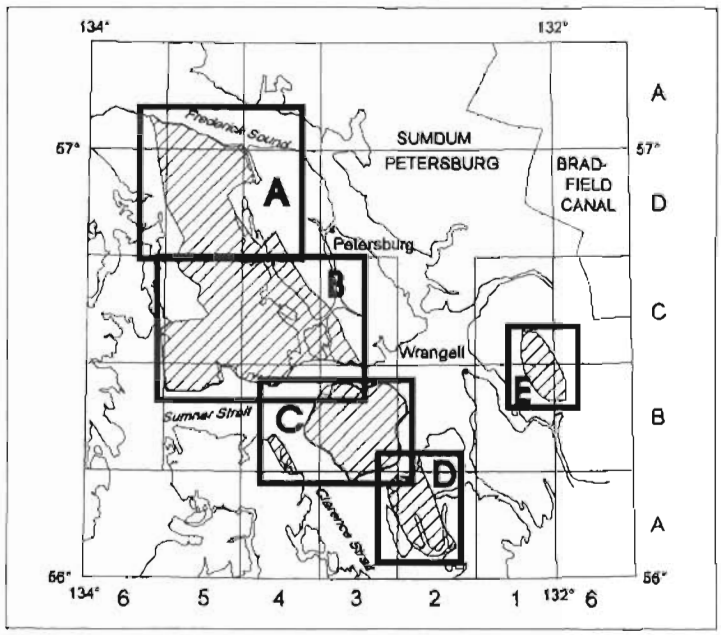

Index map for Aeromagnetic and Resistivity maps that are available at 1:63,360 scale. The aeromagnetic maps at this scale show magnetic contours and have an EM anomaly symbol denoting signal strength. The EM anomoly is derived from the coaxial coil pairs which emphasize the vertical or near vertical conductors. There is no interpretation as to the source of the EM anomaly at maps of this scale.

Location Index for scale 1:31,680

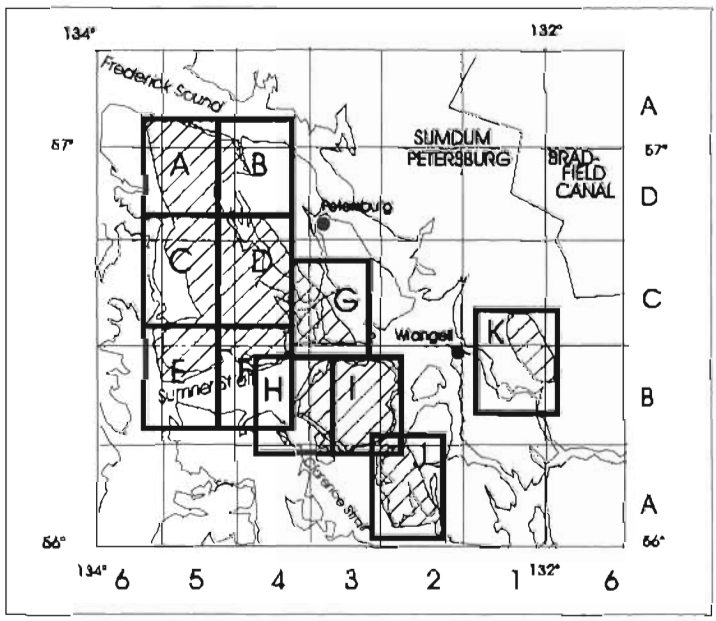

Index map for Aeromagnetic maps available at 1:31,680 scale. The aeromagnetic maps at this scale show magnetic contours and have an EM anomaly symbol denoting signal strength AND an interpretation as to what is causing the EM anomaly.

DGGS PUBLICATIONS PRODUCED FOR THE STIKINE AREA SURVEY

AEROMAGNETIC MAPS

RI 97-16A. Total field magnetics and electromagnetic anomalies of the Stikine area, Southeast Alaska, Map A - North Duncan Canal, 1 sheet, 3 colors, scale 1:63,360.

RI 97-16B. Total field magnetics and electromagnetic anomalies of the Stikine area, Southeast Alaska, Map B - South Duncan Canal, 1 sheet, 3 colors, scale 1:63,360.

RI 97-16C. Total field magnetics and electromagnetic anomalies of the Stikine area, Southeast Alaska, Map C - Zarembo Island and eastern Prince of Wales Island, 1 sheet, 3 colors, scale 1:63,360.

RI 97-16D. Total field magnetics and electromagnetic anomalies of the Stikine area, Southeast Alaska, Map D - Western Etolin Island, 1 sheet, 3 colors, scale 1:63,360.

RI 97-16E. Total field magnetics and electromagnetic anomalies of the Stikine area, Southeast Alaska, Map E - Groundhog Basin, 1 sheet, 3 colors, scale 1:63,360.

RI 97-17A. Total field magnetics of the Stikine area, Southeast Alaska, Map A - North Duncan Canal, 1 sheet, full color, scale 1:63,360. On-demand color plot from electronic file, 400 dpi. **Made on request.**

RI 97-17B. Total field magnetics of the Stikine area, Southeast Alaska, Map B - South Duncan Canal, 1 sheet, full color, scale 1:63,360. On-demand color plot from electronic file, 400 dpi. **Made on request.**

RI 97-17C. Total field magnetics of the Stikine area, Southeast Alaska, Map C - Zarembo Island and eastern Prince of Wales Island, 1 sheet, full color, scale 1:63,360. On-demand color plot from electronic file, 400 dpi. **Made on request.**

RI 97-17D. Total field magnetics of the Stikine area, Southeast Alaska, Map D - Western Etolin Island, 1 sheet, full color, scale 1:63,360. On-demand color plot from electronic file, 400 dpi. **Made on request.**

RI 97-17E. Total field magnetics of the Stikine area, Southeast Alaska, Map E - Groundhog Basin, 1 sheet, full color, scale 1:63,360. On-demand color plot from electronic file, 400 dpi. **Made on request.**

PDF 97-38A. Clear mylar version of RI 97-16A. Total field magnetics and electromagnetic anomalies of the Stikine area, Southeast Alaska, Map A - North Duncan Canal. Electromagnetic anomalies and magnetic contours 100% black; topography 50% black. 1 sheet, scale 1:63,360. **Made on request.**

PDF 97-38B. Clear mylar version of RI 97-16B. Total field magnetics and electromagnetic anomalies of the Stikine area, Southeast Alaska, Map B - South Duncan Canal. Electromagnetic anomalies and magnetic contours 100% black; topography 50% black. 1 sheet, scale 1:63,360. **Made on request.**

PDF 97-38C. Clear mylar version of RI 97-16C. Total field magnetics and electromagnetic anomalies of the Stikine area, Southeast Alaska, Map C - Zarembo Island and eastern Prince of Wales Island. Electromagnetic anomalies and magnetic contours 100% black; topography 50% black. 1 sheet, scale 1:63,360. **Made on request.**

PDF 97-38D. Clear mylar version of RI 97-16D. Total field magnetics and electromagnetic anomalies of the Stikine area, Southeast Alaska, Map D - Western Etolin Island. Electromagnetic anomalies and magnetic contours 100% black; topography 50% black. 1 sheet, scale 1:63,360. **Made on request.**

PDF 97-38E. Clear mylar version of RI 97-16E. Total field magnetics and electromagnetic anomalies of the Stikine area, Southeast Alaska, Map E - Groundhog Basin. Electromagnetic anomalies and magnetic contours 100% black; topography 50% black. 1 sheet, scale 1:63,360. **Made on request.**

PDF 97-45A-K. Total field magnetics and detailed electromagnetic anomalies of the Stikine area,

Southeast Alaska, 11 sheets, available individually, blueline, scale 1:31,680.

RESISTIVITY MAPS

RI 97-18A. 900 Hz coplanar resistivity of the Stikine area, Southeast Alaska, Map A - North Duncan Canal, 1 sheet, full color, scale 1:63,360. On-demand color plot from electronic file, 400 dpi. **Made on request.**

RI 97-18B. 900 Hz coplanar resistivity of the Stikine area, Southeast Alaska, Map B - South Duncan Canal, 1 sheet, full color, scale 1:63,360. On-demand color plot from electronic file, 400 dpi. **Made on request.**

RI 97-18C. 900 Hz coplanar resistivity of the Stikine area, Southeast Alaska, Map C - Zarembo Island and eastern Prince of Wales Island, 1 sheet, full color, scale 1:63,360. On-demand color plot from electronic file, 400 dpi. **Made on request.**

RI 97-18D. 900 Hz coplanar resistivity of the Stikine area, Southeast Alaska, Map D - Western Etolin Island, 1 sheet, full color, scale 1:63,360. On-demand color plot from electronic file, 400 dpi. **Made on request.**

RI 97-18E. 900 Hz coplanar resistivity of the Stikine area, Southeast Alaska, Map E - Groundhog Basin, 1 sheet, full color, scale 1:63,360. On-demand color plot from electronic file, 400 dpi. **Made on request.**

RI 97-19A. 7200 Hz coplanar resistivity of the Stikine area, Southeast Alaska, Map A - North Duncan Canal, 1 sheet, full color, scale 1:63,360. On-demand color plot from electronic file, 400 dpi. **Made on request.**

RI 97-19B. 7200 Hz coplanar resistivity of the Stikine area, Southeast Alaska, Map B - South Duncan Canal, 1 sheet, full color, scale 1:63,360. On-demand color plot from electronic file, 400 dpi. **Made on request.**

RI 97-19C. 7200 Hz coplanar resistivity of the Stikine area, Southeast Alaska, Map C - Zarembo Island and eastern Prince of Wales Island, 1 sheet, full color, scale 1:63,360. On-demand color plot from electronic file, 400 dpi. **Made on request.**

RI 97-19D. 7200 Hz coplanar resistivity of the Stikine area, Southeast Alaska, Map D - Western Etolin Island, 1 sheet, full color, scale 1:63,360. On-demand color plot from electronic file, 400 dpi. **Made on request.**

RI 97-19E. 7200 Hz coplanar resistivity of the Stikine area, Southeast Alaska, Map E - Groundhog Basin, 1 sheet, full color, scale 1:63,360. On-demand color plot from electronic file, 400 dpi. **Made on request.**

PDF 97-39A. 900 Hz coplanar resistivity of the Stikine area, Southeast Alaska, Map A - North Duncan Canal, 1 sheet, blueline, scale 1:63,360.

PDF 97-39B. 900 Hz coplanar resistivity of the Stikine area, Southeast Alaska, Map B - South Duncan Canal, 1 sheet, blueline, scale 1:63,360.

PDF 97-39C. 900 Hz coplanar resistivity of the Stikine area, Southeast Alaska, Map C - Zarembo Island and eastern Prince of Wales Island, 1 sheet, blueline, scale 1:63,360.

PDF 97-39D. 900 Hz coplanar resistivity of the Stikine area, Southeast Alaska, Map D - Western Etolin Island, 1 sheet, blueline, scale 1:63,360.

PDF 97-39E. 900 Hz coplanar resistivity of the Stikine area, Southeast Alaska, Map E - Groundhog Basin, 1 sheet, blueline, scale 1:63,360.

PDF 97-40A. 7200 Hz coplanar resistivity of the Stikine area, Southeast Alaska, Map A - North Duncan Canal, 1 sheet, blueline, scale 1:63,360.

PDF 97-40B. 7200 Hz coplanar resistivity of the Stikine area, Southeast Alaska, Map B - South Duncan Canal, 1 sheet, blueline, scale 1:63,360.

PDF 97-40C. 7200 Hz coplanar resistivity of the Stikine area, Southeast Alaska, Map C - Zarembo Island and eastern Prince of Wales Island, 1 sheet, blueline, scale 1:63,360.

PDF 97-40D. 7200 Hz coplanar resistivity of the Stikine area, Southeast Alaska, Map D - Western Etolin Island, 1 sheet, blueline, scale 1:63,360.

PDF 97-40E. 7200 Hz coplanar resistivity of the Stikine area, Southeast Alaska, Map E - Groundhog Basin, 1 sheet, blueline, scale 1:63,360.

DIGITAL FILES, PROJECT REPORT, PORTFOLIO, AND FLIGHT LINES

PDF 97-37A. Flight lines of the Stikine area, Southeast Alaska, Map A - North Duncan Canal, 1 sheet, blueline, scale 1:63,360.

PDF 97-37B. Flight lines of the Stikine area, Southeast Alaska, Map B - South Duncan Canal, 1 sheet, blueline, scale 1:63,360.

PDF 97-37C. Flight lines of the Stikine area, Southeast Alaska, Map C - Zarembo Island and eastern Prince of Wales Island, 1 sheet, blueline, scale 1:63,360.

PDF 97-37D. Flight lines of the Stikine area, Southeast Alaska, Map D - Western Etolin Island, 1 sheet, blueline, scale 1:63,360.

PDF 97-37E. Flight lines of the Stikine area, Southeast Alaska, Map E - Groundhog Basin, 1 sheet, blueline, scale 1:63,360.

PDF 97-41. CD-ROM digital archive files of 1997 survey data for Stikine area, Southeast Alaska.

PDF 97-42. Zip disc containing gridded files and section lines of 1997 geophysical survey data for Stikine area, Southeast Alaska.

PDF 97-43. Portfolio of aeromagnetic and resistivity maps of the Stikine area, Southeast Alaska. Includes color and shadow maps. Maps fit on 8½" x 11" sheet.

PDF 97-44. Project report of the airborne geophysical survey for Stikine area, Southeast Alaska, by Ruth Pritchard, 1997.

SOME AVAILABLE REFERENCES ON THE STIKINE AREA

Barker, Fred, 1994, Some accreted volcanic rocks of Alaska and their elemental abundances: in Plafker, George, and Berg, Henry C., eds., The Geology of Alaska: Boulder, Colorado, Geological Society of America, The Geology of North America, vol. G-1, p. 555-588.

Brew, David A., 1994, Latest Mesozoic and Cenozoic magmatism in southeastern Alaska: in Plafker, George, and Berg, Henry C., eds., The Geology of Alaska: Boulder, Colorado, Geological Society of America, The Geology of North America, vol. G-1, p. 621-656.

Brew, David A., 1997, Reconnaissance geologic map of the Petersburg A-2 quadrangle, southeastern Alaska: U.S. Geological Survey Open-File Report 97-156A, 21 p., 1 pl., scale 1:63,360.

Brew, David A., 1997, Reconnaissance geologic map of the Petersburg A-3 quadrangle, southeastern Alaska: U.S. Geological Survey Open-File Report 97-156B, 25 p., 1 pl., scale 1:63,360.

Brew, David A., 1997, Reconnaissance geologic map of the Petersburg B-1 quadrangle, southeastern Alaska: U.S. Geological Survey Open-File Report 97-156C, 20 p., 1 pl., scale 1:63,360.

Brew, David A., 1997, Reconnaissance geologic map of the Petersburg B-2 quadrangle, southeastern Alaska: U.S. Geological Survey Open-File Report 97-156D, 22 p., 1 pl., scale 1:63,360.

Brew, David A., 1997, Reconnaissance geologic map of the Petersburg B-3 quadrangle, southeastern Alaska: U.S. Geological Survey Open-File Report 97-156E, 24 p., 1 pl., scale 1:63,360.

Brew, David A., 1997, Reconnaissance geologic map of the Petersburg B-4 quadrangle, southeastern Alaska: U.S. Geological Survey Open-File Report 97-156F, 20 p., 1 pl., scale 1:63,360.

Brew, David A., 1997, Reconnaissance geologic map of the Petersburg B-5 quadrangle, southeastern Alaska: U.S. Geological Survey Open-File Report 97-156G, 19 p., 1 pl., scale 1:63,360.

Brew, David A., 1997, Reconnaissance geologic map of the Petersburg C-1 quadrangle, southeastern Alaska: U.S. Geological Survey Open-File Report 97-156H, 23 p., 1 pl., scale 1:63,360.

Brew, David A., 1997, Reconnaissance geologic map of the Petersburg C-3 quadrangle, southeastern Alaska: U.S. Geological Survey Open-File Report 97-156I, 18 p., 1 pl., scale 1:63,360.

Brew, David A., 1997, Reconnaissance geologic map of the Petersburg C-4 quadrangle, southeastern Alaska: U.S. Geological Survey Open-File Report 97-156J, 21 p., 1 pl., scale 1:63,360.

Brew, David A., 1997, Reconnaissance geologic map of the Petersburg C-5 quadrangle, southeastern Alaska: U.S. Geological Survey Open-File Report 97-156K, 18 p., 1 pl., scale 1:63,360.

Brew, David A., 1997, Reconnaissance geologic map of the Petersburg D-4 quadrangle, southeastern Alaska: U.S. Geological Survey Open-File Report 97-156L, 22 p., 1 pl., scale 1:63,360.

Brew, David A., 1997, Reconnaissance geologic map of the Petersburg D-5 quadrangle, southeastern Alaska: U.S. Geological Survey Open-File Report 97-156M, 23 p., 1 pl., scale 1:63,360.

Brew, David A., 1997, Reconnaissance geologic map of the Bradfield Canal B-6 quadrangle, southeastern Alaska: U.S. Geological Survey Open-File Report 97-156N, some text, 1 pl., scale 1:63,360.

Brew, D.A., Ovenshine, A.T., Karl, S.M., and Hunt, S.J., 1984, Preliminary reconnaissance geologic map of the Petersburg and parts of the Port Alexander and Sumdum 1:250,000 quadrangles, southeastern Alaska: U. S. Geological Survey, Open-file Report 84-405, 42 p., 1 pl., scale 1:250,000.

Bundtzen, T.K., and Henning, M.W., 1978, Barite in Alaska: AK Division of Geological & Geophysical Surveys, Miscellaneous Papers 17, Mines & Geology Bulletin, v. 27, no. 4, p. 1-4.

Combellick, R.A., and Long, W.E., 1983, Geologic hazards in southeastern Alaska: an overview: Alaska Division of Geological & Geophysical Surveys, Report of Investigations 83-17, 17 p.

Eakins, G.R., 1969, Uranium in Alaska: Alaska Division of Mines and Geology, Geologic Report 38, 49 p., scale 1:3,800,000, 1 sheet.

Eakins, G.R., 1975, Uranium investigations in southeastern Alaska: Alaska Division of Geological & Geophysical Surveys, Geologic Report 44, 62 p.

Eakins, G.R., and Forbes, R.B., 1976, Investigation of Alaska's uranium potential: Alaska Division of Geological & Geophysical Surveys, Special Report 12, 372 p., scale 1:1,000,000, 5 sheets.

Foley, J.Y., Burns, L.E., Schneider, C.L., and Forbes, R.B., 1989, Preliminary report of platinum group element occurrences in Alaska: Alaska Division of Geological & Geophysical Surveys, Public-data File 89-20, 33 p., scale 1:2,500,000, 1 sheet.

Fowler, H.M., 1948, Taylor Creek lead-zinc prospect, Duncan Canal, Kupreanof Island, Alaska: AK Territorial Dept. of Mines, Properties Examined 117-5, 1 p.

Gehrels, George E., and Berg, Henry C., 1994, Geology of southeastern Alaska: in Plafker, George, and Berg, Henry C., eds., The Geology of Alaska: Boulder, Colorado, Geological Society of America, The Geology of North America, vol. G-1, p. 451-467.

Glover, A.E., 1951, Salmon Bay - Red Bay reconnaissance, Prince of Wales Island: AK Territorial Dept. of Mines, Mineral Investigations 117-1, 6 p.

Hawley, C.C., and Clark, Allen L., 1973, Geology and mineral deposits of the Stikine-Yentna Mineral Belt, Alaska, in Geology and mineral deposits of the upper Stikine and Yentna districts, south-central Alaska: U.S. Geological Survey Professional Paper 758-A, p. A1-A10, 2 sheets; 1:250,000, 1:500,000 scale.

Hawley, C.C., and Clark, Allen L., 1974, Geology and mineral deposits of the upper Stikine District, Alaska, in Geology and mineral deposits of the upper Stikine and Yentna districts, south-central Alaska: U.S. Geological Survey Professional Paper 758B, p. B1-B47, 2 sheets, 1:48,000, 1:12,000, 1:2,400 scale.

Hodge, E.T., 1944, Southeastern coastal Alaska limestone terrain: AK Territorial Dept. of Mines, Miscellaneous Reports 191-8, 17 p., scale 1:2,000,000.

Hunt, S.J., 1986, Structural analysis of plutonic and metamorphic rocks in an area east of Wrangell, Alaska: U. S. Geological Survey Open-file Report 86-50, 25p.

Jones, D.L., Silberling, N.J., Csejtey, Béla Jr, Nelson, W.H., and Blome, Charles D., 1980, Age and structural significance of ophiolite and adjoining rocks in the Upper Stikine district, south-central Alaska, in Geologic Framework of the upper Stikine district, Alaska: U.S. Geological Survey Professional Paper 1121-A, p. A1-A21, 2 plates in text, 1 sheet, 1:63,360 scale.

Kerr, F.A., 1948, Lower Stikine and western Iskut River areas, British Columbia, Canada: Canada Geologic Surveys Memoir 246, 94 p.

Kline, J.T., and Pinney, D.S., 1995, Preliminary map of selected occurrences of industrial minerals in Alaska: Alaska Division of Geological & Geophysical Surveys, Public-Data File 95-24, 3 sheets, scale 1:2,500,000.

Liss, S.A., and Wiltse, M.A., 1993, United States Geological Survey Alaska Mineral Resource Appraisal Program (AMRAP) geochemical data for Bradfield Canal Quadrangle, Alaska: Alaska Division of Geological & Geophysical Surveys, Public-data File 93-39g, 7 p.

Liss, S.A., and Wiltse, M.A., 1993, United States Geological Survey Alaska Mineral Resource Appraisal Program (AMRAP) geochemical data for Petersburg Quadrangle, Alaska: Alaska Division of Geological & Geophysical Surveys, Public-data File 93-39u, 7 p.

Newberry, R.J., 1995, An update on skarn deposits of Alaska: Alaska Division of Geological & Geophysical Surveys Public-Data File 95-20, 72 p., 1 disk.

Patton, William W., Jr., Box, Stephen E., and Grybeck, Donald G., 1994, Ophiolites and other mafic-ultramafic complexes in Alaska: in Plafker, George, and Berg, Henry C., eds., The Geology of Alaska: Boulder, Colorado, Geological Society of America, The Geology of North America, vol. G-1, p. 671-686.

Race, W.H., 1963, Property examination report, J.W. Huff Prospect (lower east side of Nelson Glacier): AK Territorial Dept. of Mines, Properties Examined 118-3, 12 p.

Race, W.H., 1963, Castle Island barite deposit, Duncan Canal, Alaska (Petersburg Quadrangle): AK Territorial Dept. of Mines, Properties Examined 117-9, 15 p., 1 map, scale 1:480.

Robinson, M.S., and Bundtzen, T.K., , Historic gold production in Alaska - a minisummary in Mines and Geology Bulletin, v. 28, no. 3, p 1-4: Alaska Division of Geological & Geophysical Surveys, MP 28, 4 p.

Roehm, J.C., 1946, Preliminary report on Taylor Creek lead-zinc property of Ora P. Schoonover (Taylor

Creek): AK Territorial Dept. of Mines, Properties Examined 117-4, 2 p.
Shepard, J.G., 1925, The Lake Virginia Mining Company (Groundhog Basin): Alaska Territorial Dept. of Mines, Properties Examined 117-2, 1 p.
Shepard, J.G., 1925, Ground Hog Basin Claims: AK Territorial Dept. of Mines, Properties Evaluated 117-3, 4 p., 1 map.
Smith, Alexander, 1943, Report on Groundhog Basin claims, Wrangell District, Alaska: AK Territorial Dept. of Mines, Miscellaneous Reports 117-2, 16 p.
Williams, J.A., 1953, Preliminary report on Maid of Mexico Property (Woewodski Island): AK Territorial Dept. of Mines, Properties Examined 117-6, 4 p., 1 map, scale 1:63,360.
Williams, J.A., 1955, Taylor Creek, Windham Bay copper: AK Territorial Dept. of Mines, Mineral Investigations 115-2, 5 p.
Williams, J.A., 1957, Copper King Prospect, Bradfield Canal Quadrangle, Copper (Aaron Creek): AK Territorial Dept. of Mines, Properties Examined 118-2, 5 p.
Williams, J.A., and Decker, P.A., 1932, Exploring Castle Island barite deposit by Diamond Drilling, Duncan Canal: AK Territorial Dept. of Mines, Miscellaneous Reports 117-1, 47 p., 1 map, scale 1:250,000.
Wright, F.E., and Wright, C.W., 1908, The Ketchikan and Wrangell mining districts, Alaska: U. S. Geological Survey Bulletin 347, 210 p.

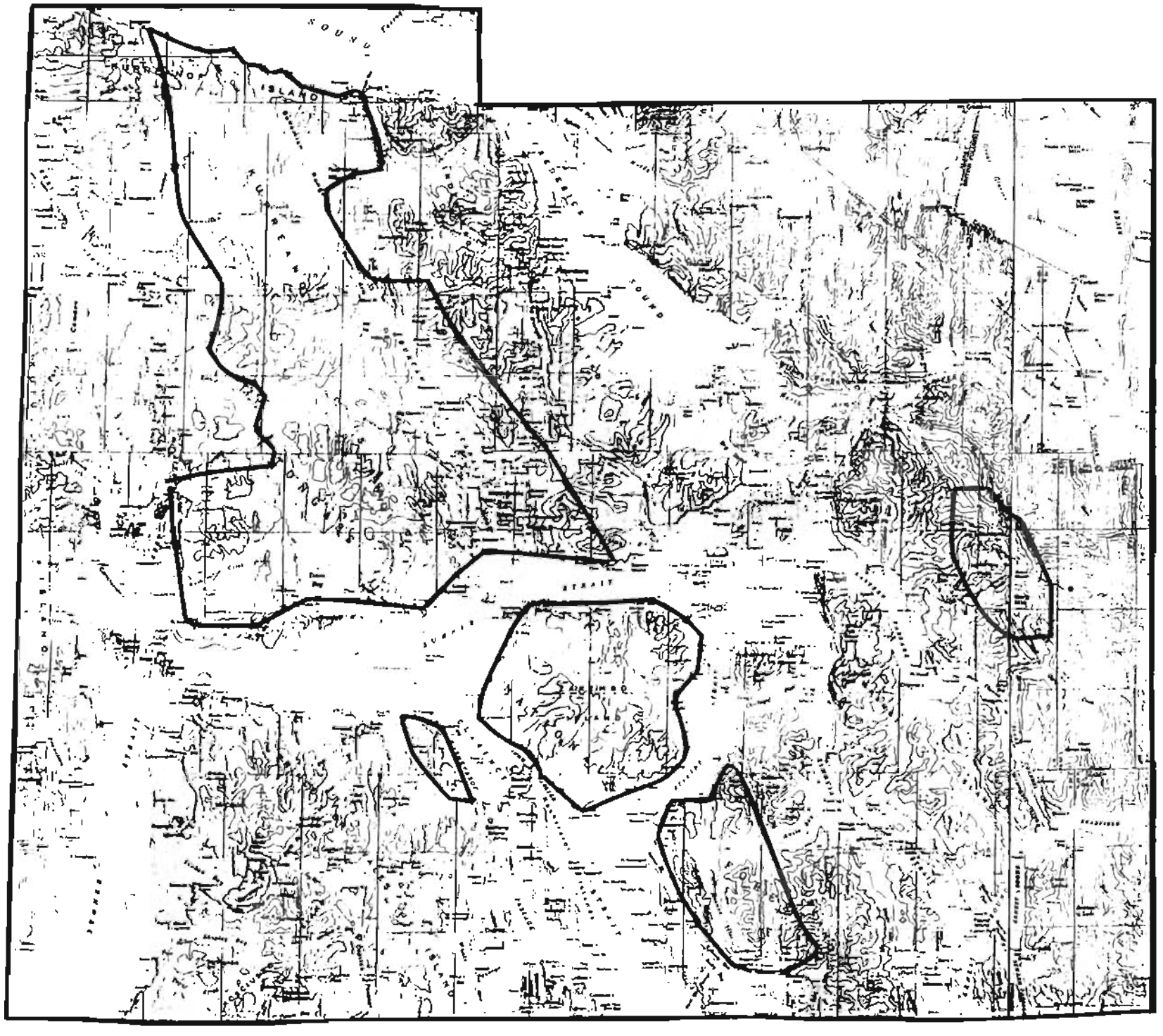

Figure 6: Survey Locations - Stikine Area - Southeast Alaska

Figure 1: Total field magnetics of the Stikine area, Southeast Alaska. Magnetic units are in nT.

Figure 2: Shadow map of the aeromagnetic data from the Stikine area, Southeast Alaska. Illumination source is at 159 degrees. High magnetic values appear like the tops of mountains that are hit by sunlight.

Figure 3: Shadow map of the aeromagnetic data from the Stikine area, Southeast Alaska. Illumination source is at 282 degrees. High magnetic values appear like the tops of mountains that are hit by sunlight.

Figure 4: 7200 Hz resistivity map of the Stikine area, Southeast Alaska. Resistivity values in ohm-m. Conductive units have low values and are shown in purple and orange on this map.

Figure 5: 900 Hz resistivity map of the Stikine area, Southeast Alaska. Resistivity values in ohm-m. Conductive units have low values and are shown in purple and orange on this map.